Virology 513 (2018) 108–113

Contents lists available at ScienceDirect

Virology

journal homepage: www.elsevier.com/locate/virology

Dynamics of lentiviral infection in vivo in the absence of adaptive immune responses

Elissa J. Schwartz[a,b,*], Naveen K. Vaidya[d], Karin S. Dorman[e,f], Susan Carpenter[g], Robert H. Mealey[c]

[a] School of Biological Sciences, Washington State University, Pullman, WA 99164, USA
[b] Department of Mathematics and Statistics, Washington State University, Pullman, WA 99164, USA
[c] Department of Veterinary Microbiology and Pathology, Washington State University, Pullman, WA 99164, USA
[d] Department of Mathematics and Statistics, San Diego State University, San Diego, CA 92182, USA
[e] Department of Statistics, Iowa State University, Ames, IA 50011, USA
[f] Department of Genetics, Development and Cell Biology, Iowa State University, Ames, IA 50011, USA
[g] Department of Animal Science, Iowa State University, Ames, IA 50011, USA

ARTICLE INFO

Keywords:
Virus dynamics
EIAV
SCID
Mathematical modeling
Kinetic parameter estimation
Neutralizing antibody efficacy

ABSTRACT

Understanding the dynamics of acute viral infection is crucial for developing strategies to prevent and control infection. In this study, lentiviral dynamics in a host without adaptive immunity were examined in order to determine kinetic parameters of infection and quantify the effect of neutralizing antibodies in preventing infection, using mathematical modeling of data from equine infectious anemia virus (EIAV) infection of horses with severe combined immunodeficiency (SCID). Estimated parameters were used to calculate the basic reproductive number and virus doubling time and found that the rate that antibodies neutralized virus was ~18 times greater than the virus clearance rate. These results establish EIAV replication kinetics in SCID horses and the minimal efficacy of antibodies that blocked infection. Furthermore, they indicate that EIAV is at most mildly cytopathic. This study advances our understanding of EIAV infection and may have important implications for the control of other viral infections, including HIV.

1. Introduction

The dynamics of acute lentivirus infection have not been fully understood. In particular, viral kinetics independent of adaptive immune responses have not been elucidated but can inform effective vaccine development. Here we determine estimates of kinetic parameters of acute lentivirus infection in a host without adaptive immunity and quantify the effects of antibody infusions that prevented viral infection. Equine infectious anemia virus (EIAV) is a macrophage-tropic lentivirus that establishes a persistent infection in horses and ponies (Issel et al., 2014; Maury and Oaks, 2010). While EIAV infection typically induces an effective adaptive immune response including cytotoxic T lymphocytes (CTL) and antibodies (Cook et al., 2013; Mealey et al., 2005, 2003), horses with severe combined immunodeficiency (SCID) lack functional B and T lymphocytes and therefore completely lack the ability to mount these responses to infection (Taylor et al., 2010, 2011). Thus, kinetic analysis of EIAV dynamics in SCID horses provides a unique opportunity to study the dynamics of viral infection and to estimate infection kinetics in the absence of CTL and antibody involvement. Using these results, we are able to quantify the efficacy of neutralizing antibody infusions that can block infection.

Our previous studies document the time course of early EIAV infection in SCID horses and demonstrate the protection from infection of a SCID horse by passive transfer of broadly neutralizing antibodies (Taylor et al., 2010; Mealey et al., 2008). In the present study, EIAV infection dynamics in these SCID horses were examined using mathematical modeling in order to investigate viral growth kinetics in the absence of adaptive immunity and to estimate the effect of the antibodies that inhibited infection. The kinetic estimates were used to calculate the basic reproductive number, virus doubling time, and steady state values for viral load, uninfected target cells, and infected cells. Due to the availability of this rare data set of viral loads in the complete absence of T and B cell-mediated immune responses, this study provides estimates of key parameters of lentivirus dynamics in vivo without the interference of adaptive immunity. Such estimates may have considerable implications for understanding the dynamics of other lentiviral infections, including human immunodeficiency virus (HIV-1) (Cook et al., 2013; Sponseller et al., 2007). Moreover, our

* Correspondence to: School of Biological Sciences and Department of Mathematics and Statistics, Washington State University, P.O. Box 643113, Pullman, WA, USA.
E-mail address: ejs@wsu.edu (E.J. Schwartz).

http://dx.doi.org/10.1016/j.virol.2017.09.023
Received 8 May 2017; Received in revised form 25 September 2017; Accepted 26 September 2017

estimate of the efficacy of infused antibodies that can prevent infection may be useful in vaccine development.

2. Methods

To mathematically model the viral load data, the following basic model of viral infection was considered (Perelson and Ribeiro, 2013; Neumann et al., 1998; Nowak and Bangham, 1996; Perelson et al., 1996):

$$\frac{dM}{dt} = \lambda - \rho M - \beta MV$$

$$\frac{dI}{dt} = \beta MV - (\delta + \sigma)I$$

$$\frac{dV}{dt} = bI - (\gamma + \alpha)V$$

The target cells of EIAV infection are primarily tissue macrophages (Harrold et al., 2000; Oaks et al., 1998; Sellon et al., 1992). Uninfected target cells are represented by M. The model assumes that these cells become infected cells (I) at rate β following contact with EIAV (V). Infected cells produce virus at rate b; the model accommodates the possibility that viral particles either bud or burst. Uninfected target cells arise at rate λ and die at rate ρ. Infected cells die at rate δ, and virus is cleared at rate γ. We introduce σ and α to represent the effects of infected cell killing by CTLs and virus cleared by neutralizing antibodies, respectively.

To determine the values of the model parameters, we fit the model to plasma viral load data from seven Arabian SCID horses experimentally infected with EIAV (see Supplementary Material) (Taylor et al., 2010; Mealey et al., 2008). For each horse, the model was fit to data on plasma viral load using nonlinear least squares data fitting, as described previously (Vaidya et al., 2010). Viral load measurements were taken beginning the initial day of infection through 4–6 weeks post-infection with sampling every few days. As part of previous studies, horses A2245 and A2247 received infusions of irrelevant control antibodies from an uninfected immunocompetent horse (Taylor et al., 2010), and horses A2193, A2199, A2202, A2205, and A2217 received infusions of EIAV-specific CTL clones that did not engraft (Mealey et al., 2008). Thus all of these SCID horses were completely devoid of all EIAV-specific adaptive immunity. Therefore, we take the infected cell killing by CTLs and the virus clearance by neutralizing antibodies equal to zero (i.e., $\sigma = \alpha = 0$) for these seven horses. An eighth horse (horse A2241) was infused with plasma containing EIAV-specific neutralizing antibodies from a long-term EIAV-infected immunocompetent horse, which protected horse A2241 from EIAV challenge (see Supplementary Material) (Taylor et al., 2010). As this horse showed protection from infection due to EIAV-specific antibodies, we used $\sigma = 0$ and $\alpha > 0$ to model viral dynamics in this horse. All experiments involving animals in these previously published studies were approved by the Washington State University Institutional Animal Care and Use Committee.

We carried out an analysis to determine whether the model parameters we expect to estimate are uniquely identifiable for the available EIAV viral load data. Based upon estimates derived from previous experimental studies (see Table 1 footnote 2), we fixed the values of two model parameters, λ (the uninfected target cell recruitment rate) and ρ (the uninfected target cell death rate). Using the techniques of Wu et al. (2008), we found that with λ fixed and at least eight viral load (V) data points, five parameters (β, ρ, δ, γ, b) of our model can be uniquely estimated. Since we fixed ρ using previously available data, and as we have greater than eight viral load data points (average number of data points per horse = 11), identifying four parameters, δ (the death rate of infected cells), β (the infection rate), b (the virus production rate), and γ (the virus clearance rate), in this study is feasible and does not violate the conditions required for unique parameter identifiability.

3. Results

Parameter estimates for infection rate (β), death rate of infected cells (δ), virus production rate (b), and viral clearance rate (γ) were determined for each unprotected horse. These parameter estimates, along with 95% confidence intervals and the median values across all horses, are given in Table 1. Of note, these values were calculated with the benefit of frequent sampling during early infection (median number of data points before viral peak = 12). To our knowledge, no similar study has included this many data points before peak viremia in acute infection. Furthermore, these parameter estimates are independent of the contributions of adaptive immune mechanisms such as CTL killing, neutralization by antibodies, and inhibition by CD8-derived soluble factors (Cocchi et al., 1995; Klatt et al., 2010; Levy, 2015; Mosoian et al., 2010; Saksena et al., 2008). Previously, an appropriate data set that could be utilized to yield quantitative estimates of infection kinetics in the absence of adaptive immunity was unavailable.

Fits of the model (lines) to the data (points) are shown in Fig. 1. There is excellent agreement between the model and the data. The model fits identified a trend in the dynamics in which the viral load increased exponentially and then saturated, reaching a plateau (or steady state) at the peak virus load, around 10^6 or 10^7 vRNA copies/ml. Notably, it is a valid question why virus replication does not continue to increase in the absence of adaptive immune responses. These trends indicate that adaptive immunity is not essential to limit the exponential viral growth during acute EIAV infection in SCID horses. The leveling off of the growth could be due to target cell limitation or innate immune responses.

The median estimate for the infected cell death rate, δ, was 0.057/day, which indicates that infected cells turned over in about 18 days, implying only a slight reduction in cell lifespan due to infection, since uninfected cells turn over in 21 days (ρ = 0.048/day (Valli, 2007), Table 1). Because the confidence interval for δ includes 0.048 in six of the seven horses, we also report parameter estimates obtained assuming equal infected and uninfected cell death rates (i.e., $\delta = \rho = 0.048$/day) (Table 1). There was little evidence against this constrained model in any of the horses (F-test p-value > 0.05 for each horse). Therefore, all subsequent results are shown for the model assuming equal death rates $\delta = \rho = 0.048$/day. Model simulations using these median values from Table 1 are shown in Fig. 1 (bottom right panel). Together, these results imply that EIAV infection in SCID horses is at most mildly cytopathic, certainly less cytopathic than other lentiviruses studied in immunocompetent hosts (Stafford et al., 2000). A modest cytopathicity is plausible because the evidence for macrophage cytopathicity caused by EIAV in vivo is not definitive, and SCID horses lack CTLs to kill infected cells. In vitro, EIAV can kill some of the cell types it infects but not others (Maury et al., 2003; Rasty et al., 1990). In vivo, the extent of EIAV-induced infected cell lysis in either SCID or immunocompetent hosts needs further study.

The basic reproductive number, R_0, which indicates the average number of cells infected by a single infected cell when uninfected cells are not limiting (Stafford et al., 2000; Bonhoeffer et al., 1997), was calculated to be

$$R_0 = \frac{\lambda\beta b}{(\delta + \sigma)(\gamma + \alpha)\rho}$$

Values for R_0 for each unprotected horse ($\sigma = \alpha = 0$; i.e., no infected cell killing by CTLs (σ) nor virus clearance by neutralizing antibodies (α)) are shown in Table 2; the median value was 18.8. According to mathematical theory (Ribeiro et al., 2010), a value of $R_0 > 1$ indicates that the infection establishes, consistent with the data. Another SCID horse A2241 (see Supplementary Material), which was infused with broadly neutralizing antibodies from a long-term EIAV-infected immunocompetent horse (Taylor et al., 2010), however, showed no viral load and was protected from infection. The data from this horse clearly indicate that the infection was prevented, implying $R_0 < 1$. Note

Table 1
Estimates of kinetic parameters of infection.[a,b]

Horse	Infection rate,β ($\times 10^{-7}$) (ml/(vRNA copies*day))	Infected cell death rate,δ (/day)	Virus production rate,b (vRNA copies/(cell*day))	Virus clearance rate,γ (/day)
A2245	0.94 (0.88–1.00)	0.06 (0.04–0.07)	2124 (2122–2125)	16.84 (16.65–17.04)
A2247	1.98 (1.73–2.24)	0.06 (0.05–0.066)	889 (879–898)	10.88 (9.58–12.17)
A2193	4.08 (2.31–5.85)	0.05 (0.01–0.09)	870 (849–890)	16.91 (13.73–20.08)
A2199	3.20 (1.18–5.23)	0.06 (0–0.58)	746 (670–823)	9.01 (1.21–16.78)
A2202	1.77 (1.29–2.23)	0.06 (0.010–0.11)	1294 (1281–1307)	9.60 (7.81–11.39)
A2205	4.52 (3.46–5.58)	0.07 (0.02–0.12)	507 (500–513)	10.01 (9.22–10.77)
A2217[c]	5.40 (2.68–8.12)	0.07 (0.00–0.13)	101 (91–108)	2.85 (1.58–4.12)
Median (IQR)	3.20 (1.88–4.3)	0.06 (0.06–0.06)	870 (626.5–1091.5)	10.01 (9.31–13.86)
Estimates of kinetic parameters with $\delta = \rho = 1/21$				
A2245	0.94 (0.89–0.99)	1/21	2267 (2265–2268)	17.82 (17.68–17.95)
A2247	2.11 (1.82–2.39)	1/21	505 (503–508)	6.73 (6.62–6.84)
A2193	4.06 (3.51–4.60)	1/21	846 (842–849)	16.31 (15.88–16.73)
A2199	3.25 (2.16–4.33)	1/21	646 (615–676)	8.02 (4.82–11.22)
A2202	1.86 (1.25–2.47)	1/21	379 (373–386)	2.82 (2.28–3.35)
A2205	5.09 (2.35–7.84)	1/21	108 (100–115)	2.33 (1.06–3.59)
A2217[c]	5.91 (4.51–7.32)	1/21	92 (86–97)	2.94 (2.52–3.35)
Median (IQR)	3.25 (1.99–4.58)	1/21	505 (244–746)	6.73 (2.88–12.17)

[a] Values and 95% confidence intervals (in parentheses) were determined using DEDiscover software (http://www.dediscover.org).

[b] The fixed parameters λ (uninfected target cell recruitment rate) and ρ (uninfected target cell death rate) were set as follows: The value for λ, 2019 cells/(ml*day), was calculated using $\lambda = \rho * M_0$ (where M_0 is the initial number of uninfected target cells (i.e., tissue macrophages)), as it is assumed that $dM/dt = 0$ before infection. The value for ρ, 1/21 per day, was calculated using the estimate for a macrophage lifespan of 21 days (Valli, 2007). The value for M_0 was estimated to be 42390 cells/ml as follows: Because this cell population arises from monocytes in the circulation that enter the tissue and differentiate into macrophages, the average monocyte count in the peripheral blood of 4 SCID horses (measured as 353.25 cells/μl (Mealey et al., 2008)) was multiplied by the rate of monocyte turnover in one day (due to dying or differentiating into tissue macrophages), which is 0.12 (Hasegawa et al., 2009). All animals were inoculated IV with 10^6 $TCID_{50}$ $EIAV_{WSU5}$, a cell culture-adapted strain derived originally from wild-type $EIAV_{Wyo}$ (Taylor et al., 2010; Mealey et al., 2008). The number of vRNA copies that established infection, V_0, 467 copies/ml, was estimated from the initial inoculum of infectious virus (10^6 $TCID_{50}$) and the plasma volume of the horses (3 L, as the horses weighed ~ 60 kg at the time of the experiment and plasma volume is 5% of body weight) using the conversion factor between $TCID_{50}$ and plaque forming units (PFU) of 0.7 (Bryan, 1957), and given 2 copies of RNA in each viral particle. The initial number of infected cells, I_0, was 0 cells/ml. Studies presume proportionate measurements between blood and tissue.

[c] Previously unreported data (see Supplementary Material).

that for this horse, $\sigma = 0$ and $\alpha > 0$. Comparison of R_0 between unprotected horses and the protected horse allows us to estimate α, the effect of infused neutralizing antibodies on clearing the virus, to be greater than 17.8 times higher (median value; range 9.6–22.3) than the virus clearance rate γ.

Other kinetic estimates predicted by the model are also provided (Table 2). The virus doubling time, estimated from the exponential growth rate, was 1.0 day. Steady state values for viral load (V^*), infected cells (I^*), and uninfected target cells (M^*) were calculated from the model steady state solutions and evaluated at parameter values. Steady state viral loads were predicted to range between 10^6 to 10^7 RNA copies/ml in the unprotected SCID horses. The total cell loss, as calculated from the initial sum $M_0 + I_0$ and the steady state sum $M^* + I^*$, was 0.07%. This mild target cell destruction due to infection is in accordance with the lack of cytopathicity of EIAV discussed above. Other values calculated here are similar to those reported for other lentiviral infections such as HIV-1 and simian immunodeficiency virus (SIV). Specifically, the value for R_0 for EIAV (median 18.8; IQR 15.3 – 21.6) falls within the ranges reported for HIV (5.7 – 19.3) (Stafford et al., 2000; Ribeiro et al., 2010; Althaus et al., 2009; Little et al., 1999) and SIV (3.6 – 36.5) (Nowak et al., 1997). EIAV doubling time (median 1 day; IQR 0.88 – 1.18) is not far greater than that reported for HIV (median 0.65 day; IQR 0.56 – 0.91) (Ribeiro et al., 2010). Steady state levels for EIAV log virus load that we calculate here (6.47 RNA copies/ml) are within an order of magnitude of that reported for HIV (5.26 RNA copies/ml) (Stafford et al., 2000).

The parameter estimates were obtained assuming known values for the target cell death rate (ρ), the initial number of susceptible target cells (M_0), and the initial virus load (V_0) (Table 1). There is uncertainty in these values, so we conducted a sensitivity analysis in order to determine their effect on our parameter estimates. Changing the parameter ρ affects the estimates of parameters for the infection rate (β), the viral production rate (b), and the viral clearance rate (γ), and changing M_0 affects the estimate of b, while the other parameters are unaffected (Table 3). When we considered an initial viral load (V_0) 10-fold lower and 10-fold higher than the base value, parameter estimates were not significantly altered (Table 3). Furthermore, we allowed V_0 to be a free parameter in our fitting process. In this case, we did not find significant improvement in fitting the data, and the estimated V_0 appeared to be approximately the same as the base value. In all these sensitivity analyses, we found that the estimated values do not vary greatly compared to our previous estimates.

Using our model, we next calculated the infectivity of EIAV in vivo. In terms of the fixed parameter for the initial number of uninfected target cells 42390 cells/ml, and estimated parameters for infection rate $\beta = 10^{-7}$ ml/(vRNA copies*day) and viral clearance rate $\gamma = 6.73$/day, the number of infected cells per RNA copy in a single cycle in vivo on average is given by $\beta M_0/\gamma = 2.05 \times$ cells/RNA copy. Equivalently, 205 out of 100,000 viral RNA copies infect a cell. It is interesting to note that the infectivity in vivo estimated here is similar to that reported by Wu et al. (2011) for infectivity in vitro, despite differences between these studies. Wu et al. performed infectivity assays for EIAV by counting focus forming units (FFU), and estimated that 38 out of 100,000 viral RNA copies successfully infect a cell in a single cycle in vitro.

4. Discussion

This study combines mathematical modeling with a unique viral load data set from immunodeficient animals, allowing us to establish kinetic parameters of infection in the absence of specific immune responses and the minimal efficacy of infused antibodies that prevented infection. Furthermore, this study found EIAV to be at most mildly cytopathic. This study and its findings are different from previous viral dynamics studies in that not only is it uncommon to have such frequent viral load data from acute infection, but also most other kinetics reported (Vaidya et al., 2010; Stafford et al., 2000; Ribeiro et al., 2010) have been estimated from viral infection data that included the effects of adaptive immune responses without knowledge about the magnitude of the effects of these immune responses. The finding that viral load,

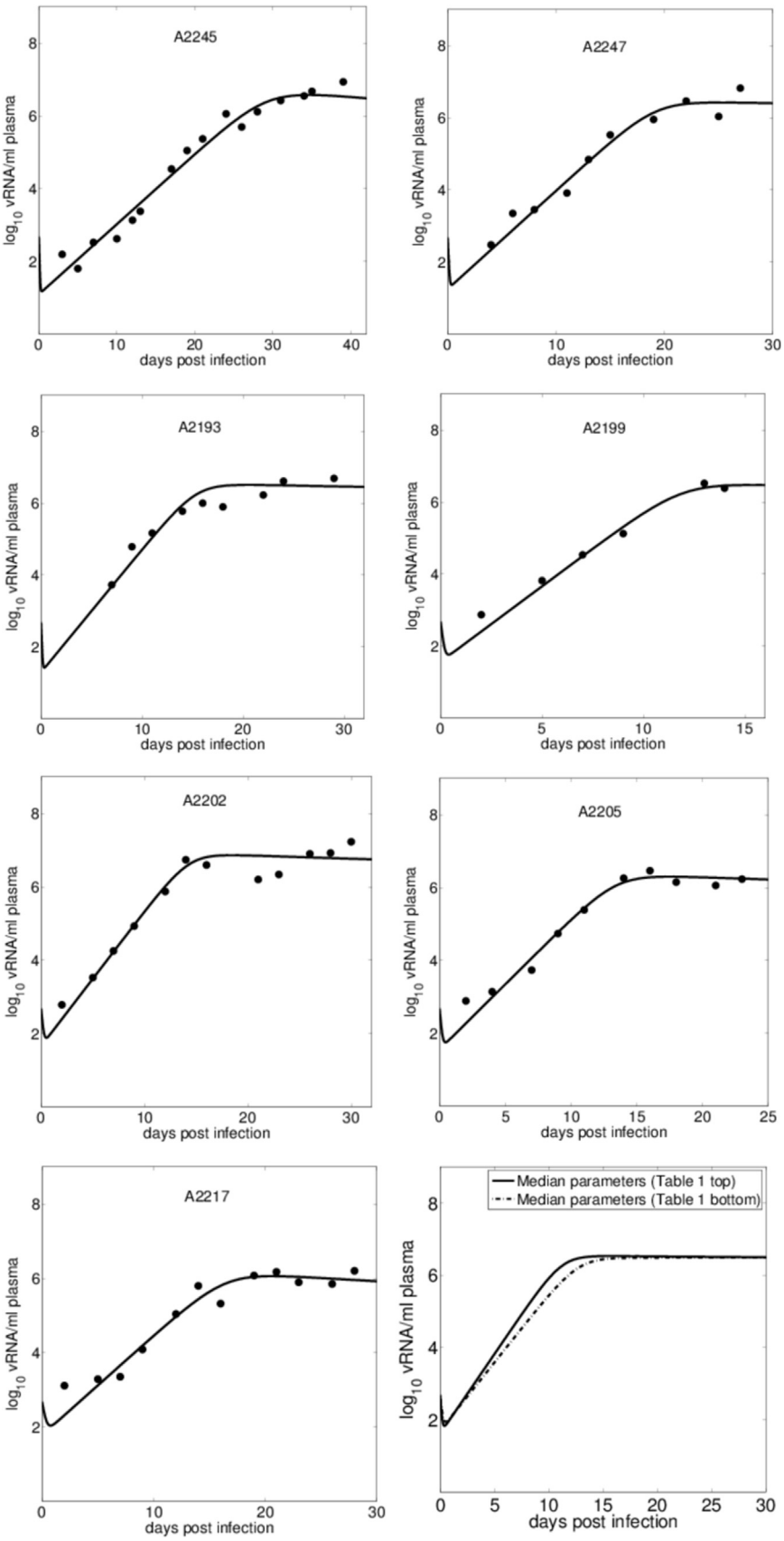

Fig. 1. Results of fitting model to viral load data in EIAV-infected Arabian SCID horses. Data (points); model (lines). Bottom right panel: model simulation using median values from Table 1.

Table 2
Basic reproductive numbers (R0), exponential growth rates (r), virus doubling times (t_2), steady state uninfected target cell levels (M^*), steady state infected cell levels (I^*), and steady state viral loads (V^*) for each horse.[a]

Horse	R_0	r (/day)	t_2 (day)	M^* ($\times 10^3$) (cells/ml)	I^* ($\times 10^4$) (cells/ml)	$log_{10}(V^*)$ (RNA copies/ml)
A2245	10.6	0.45	1.6	3.99	3.84	6.69
A2247	14.1	0.57	1.2	3.01	3.94	6.47
A2193	18.8	0.80	0.9	2.26	4.01	6.32
A2199	23.3	0.95	0.7	1.82	4.06	6.51
A2202	22.3	0.78	0.9	1.90	4.05	6.74
A2205	21.0	0.72	1.0	2.02	4.04	6.27
A2217	16.5	0.60	1.1	2.57	3.98	6.10
Median (IQR)	18.8 (15.3–21.6)	0.72 (0.59–0.79)	1.0 (0.88–1.18)	2.26 (1.96–2.79)	4.01 (3.96–4.04)	6.47 (6.30–6.60)

[a] Estimates assume equal uninfected cell and infected cell death rates, i.e., $\delta = \rho = 1/21$ (as in Table 1 bottom).

Table 3
Sensitivity analysis using a range of values for uninfected cell death rate, ρ (/day),[a] initial uninfected cell number, M_0 (cells/ml),[b] and initial viral load, V_0 (vRNA copies/ml),[c] to compute sensitivity to parameters β (infection rate), b (virus production rate), and γ (virus clearance rate). Values shown are for horse A2193, which was representative of the patterns seen in all horses.

Parameter	β ($\times 10^{-7}$)	b	γ
ρ			
0.1	4.58	1024	20.35
0.048	4.06	846	16.31
0.023	4.05	574	11.52
0.0058	2.62	166	3.06
M_0			
32,852	4.06	1092	16.31
42,390	4.06	846	16.31
57,580	4.06	623	16.31
353,250	4.06	102	16.31
500,000	4.06	72	16.31
V_0			
46.7	6.14	846	18.88
467	4.06	846	16.31
4670	2.02	846	11.40

[a] Values were chosen as follows: The estimate of 21 days for the lifespan of a Kupffer cell (liver macrophage) in mice (Valli, 2007) gives ρ = 1/21 = 0.048. The estimates of 30 days and 120 days for the half-life of alveolar macrophages in mice (Murphy et al., 2008) give ρ = ln2/30 = 0.023 and ρ = ln2/120 = 0.0058, respectively. All results assume equal death rates of uninfected and infected cells, i.e., $\delta = \rho$. Other fixed values were as described (Table 1) except the calculation of the uninfected target cell recruitment rate, λ = $\rho^* M_0$.

[b] Values for M_0 were chosen as follows: The value 32,852 was calculated as before (see Table 1) using the minimum value measured, 0.093/day (Hasegawa et al., 2009), for the monocyte turnover rate; the value 42,390 was calculated using the median value measured (0.12/day), and the value 57,580 was calculated using the maximum value measured, 0.163/day (Hasegawa et al., 2009), for the monocyte turnover rate; the value 353,250 equals the average monocyte count in the peripheral blood of 4 SCID horses (Mealey et al., 2008), without taking into account monocyte turnover; and the value 500,000 was calculated given a horse with 10,000,000 PBMC of which 5% are monocytes/macrophages (Carrick and Begg, 2008; Giguere et al., 2003). All estimates assume equal death rates of uninfected and infected cells, i.e., $\delta = \rho$. Other fixed values were as described (Table 1) except the calculation of the uninfected target cell recruitment rate, λ = $\rho^* M_0$.

[c] For the sensitivity of V_0, we considered a 10-fold lower and 10-fold higher viral load than the base case, 467 vRNA copies/ml, which was calculated, which was calculated as before (see Table 1). Other fixed values were as described (Table 1).

after an initial exponential growth, plateaus, indicates that factors other than adaptive host immune responses, such as innate immunity or a lack of susceptible cells, can play a role in the slowing of virus growth in acute infection. Future studies that delineate the roles of these different factors can lead to a more complete understanding of the resolution and control of acute lentiviral infection.

Some limitations on our parameter estimates should be noted. Our results assume that all tissue macrophages (M) are susceptible to infection. We also assumed that the recruitment of target cells, λ, remained constant, as in other studies (Perelson and Ribeiro, 2013; Neumann et al., 1998; Nowak and Bangham, 1996; Perelson et al., 1996; Stafford et al., 2000). In vivo, however, an influx of macrophages may result from infection. Inaccuracies in these assumptions, as well as differences in EIAV strain or dose, may lead to variation in our reported parameter values.

This report also quantifies the effect that antibodies had in preventing EIAV infection. Our estimate that α, the rate at which neutralizing antibodies cleared the virus (thereby preventing infection), was at least 17.8-fold greater than the virus clearance rate (γ) indicates that when antibody neutralization is this order of magnitude greater than virus clearance, it can be sufficient to block infection. This estimate of the minimal efficacy of infused antibodies that successfully prevented infection may be useful in vaccine development.

5. Conclusions

In summary, this study, made possible by this unique data set, determines EIAV replication kinetics in SCID horses, giving kinetic estimates of lentiviral dynamics in vivo in the absence of cellular or humoral immunity. This work also quantifies the functional effect of infused antibodies in preventing EIAV infection. These results add to our understanding of the dynamics of viral infection and may have implications for the control of other viral infections, such as HIV-1.

Acknowledgements

This work was supported in part by a seed grant from Washington State University and an award from the Mathematical Biosciences Institute NSF-DMS 0931642 (EJS), start-up funding from San Diego State University College of Sciences and NSF grant DMS-1616299 (NKV), and U.S. Public Health Service National Institutes of Health grants CA128568 (SC) and AI073101 (RHM).

Appendix A. Supplementary Material

Supplementary data associated with this article can be found in the online version at http://dx.doi.org/10.1016/j.virol.2017.09.023.

References

Althaus, C.L., De Vos, A.S., De Boer, R.J., 2009. Reassessing the human immunodeficiency virus type 1 life cycle through age-structured modeling: life span of infected cells, viral generation time, and basic reproductive number, R_0. J. Virol. 83, 7659–7667.
Bonhoeffer, S., May, R.M., Shaw, G.M., Nowak, M.A., 1997. Virus dynamics and drug therapy. Proc. Natl. Acad. Sci. USA 94, 6971–6976.
Bryan, W.R., 1957. Interpretation of host response in quantitative studies on animal viruses. Ann. N.Y. Acad. Sci. 69, 698–728.
Carrick, J.B., Begg, A.P., 2008. Peripheral blood leukocytes. The Veterinary Clinics of North America. Vet. Clin. North Am. Equine Pract. 24, 239–259.
Cocchi, F., DeVico, A.L., Garzino-Demo, A., Arya, S.K., Gallo, R.C., Lusso, P., 1995. Identification of RANTES, MIP-1 alpha, and MIP-1 beta as the major HIV-suppressive factors produced by CD8+ T cells. Science 270, 1811–1815.
Cook, R.F., Leroux, C., Issel, C.J., 2013. Equine infectious anemia and equine infectious anemia virus in 2013: a review. Vet. Microbiol. 167, 181–204.
Giguere, S., Hernandez, J., Gaskin, J., Miller, C., Bowman, J.L., 2003. Evaluation of white blood cell concentration, plasma fibrinogen concentration, and an agar gel

immunodiffusion test for early identification of foals with Rhodococcus equi pneumonia. J. Am. Vet. Med. Assoc. 222, 775–781.
Harrold, S.M., Cook, S.J., Cook, R.F., Rushlow, K.E., Issel, C.J., Montelaro, R.C., 2000. Tissue sites of persistent infection and active replication of equine infectious anemia virus during acute disease and asymptomatic infection in experimentally infected equids. J. Virol. 74, 3112–3121.
Hasegawa, A., Liu, H., Ling, B., Borda, J.T., Alvarez, X., Sugimoto, C., Vinet-Oliphant, H., Kim, W.K., Williams, K.C., Ribeiro, R.M., Lackner, A.A., Veazey, R.S., Kuroda, M.J., 2009. The level of monocyte turnover predicts disease progression in the macaque model of AIDS. Blood 114, 2917–2925.
Issel, C.J., Cook, R.F., Mealey, R.H., Horohov, D.W., 2014. Equine infectious anemia in 2014: live with it or eradicate it? The Veterinary clinics of North America. Vet. Clin. North Am. Equine Pract. 30, 561–577.
Klatt, N.R., Shudo, E., Ortiz, A.M., Engram, J.C., Paiardini, M., Lawson, B., Miller, M.D., Else, J., Pandrea, I., Estes, J.D., Apetrei, C., Schmitz, J.E., Ribeiro, R.M., Perelson, A.S., Silvestri, G., 2010. CD8+ lymphocytes control viral replication in SIVmac239-infected rhesus macaques without decreasing the lifespan of productively infected cells. PLoS Pathog. 6, e1000747.
Levy, J.A., 2015. Discovery of another anti-HIV protein in the search for the CD8+ cell anti-HIV factor. Proc. Natl. Acad. Sci. USA 112, 7888–7889.
Little, S.J., McLean, A.R., Spina, C.A., Richman, D.D., Havlir, D.V., 1999. Viral dynamics of acute HIV-1 infection. J. Exp. Med. 190, 841–850.
Maury, W., Oaks, J.L., 2010. Equine infectious anemia virus pathogenesis and replication. In: Desport, M. (Ed.), Lentiviruses and Macrophages: Molecular and Cellular Interactions. Caister Academic Press, Norfolk, UK, pp. 251–276.
Maury, W., Wright, P.J., Bradley, S., 2003. Characterization of a cytolytic strain of equine infectious anemia virus. J. Virol. 77, 2385–2399.
Mealey, R.H., Zhang, B., Leib, S.R., Littke, M.H., McGuire, T.C., 2003. Epitope specificity is critical for high and moderate avidity cytotoxic T lymphocytes associated with control of viral load and clinical disease in horses with equine infectious anemia virus. Virology 313, 537–552.
Mealey, R.H., Sharif, A., Ellis, S.A., Littke, M.H., Leib, S.R., McGuire, T.C., 2005. Early detection of dominant Env-specific and subdominant Gag-specific CD8+ lymphocytes in equine infectious anemia virus-infected horses using major histocompatibility complex class I/peptide tetrameric complexes. Virology 339, 110–126.
Mealey, R.H., Littke, M.H., Leib, S.R., Davis, W.C., McGuire, T.C., 2008. Failure of low-dose recombinant human IL-2 to support the survival of virus-specific CTL clones infused into severe combined immunodeficient foals: lack of correlation between in vitro activity and in vivo efficacy. Vet. Immunol. Immunopathol. 121, 8–22.
Mosoian, A., Teixeira, A., Burns, C.S., Sander, L.E., Gusella, G.L., He, C., Blander, J.M., Klotman, P., Klotman, M.E., 2010. Prothymosin-alpha inhibits HIV-1 via Toll-like receptor 4-mediated type I interferon induction. Proc. Natl. Acad. Sci. USA 107, 10178–10183.
Murphy, J., Summer, R., Wilson, A.A., Kotton, D.N., Fine, A., 2008. The prolonged life-span of alveolar macrophages. Am. J. Respir. Cell Mol. Biol. 38, 380–385.
Neumann, A.U., Lam, N.P., Dahari, H., Gretch, D.R., Wiley, T.E., Layden, T.J., Perelson, A.S., 1998. Hepatitis C viral dynamics in vivo and the antiviral efficacy of interferon-alpha therapy. Science 282, 103–107.
Nowak, M.A., Bangham, C.R., 1996. Population dynamics of immune responses to persistent viruses. Science 272, 74–79.
Nowak, M.A., Lloyd, A.L., Vasquez, G.M., Wiltrout, T.A., Wahl, L.M., Bischofberger, N., Williams, J., Kinter, A., Fauci, A.S., Hirsch, V.M., Lifson, J.D., 1997. Viral dynamics of primary viremia and antiretroviral therapy in simian immunodeficiency virus infection. J. Virol. 71, 7518–7525.
Oaks, J.L., McGuire, T.C., Ulibarri, C., Crawford, T.B., 1998. Equine infectious anemia virus is found in tissue macrophages during subclinical infection. J. Virol. 72, 7263–7269.
Perelson, A.S., Ribeiro, R.M., 2013. Modeling the within-host dynamics of HIV infection. BMC Biol. 11, 96.
Perelson, A.S., Neumann, A.U., Markowitz, M., Leonard, J.M., Ho, D.D., 1996. HIV-1 dynamics in vivo: virion clearance rate, infected cell life-span, and viral generation time. Science 271, 1582–1586.
Rasty, S., Dhruva, B.R., Schiltz, R.L., Shih, D.S., Issel, C.J., Montelaro, R.C., 1990. Proviral DNA integration and transcriptional patterns of equine infectious anemia virus during persistent and cytopathic infections. J. Virol. 64, 86–95.
Ribeiro, R.M., Qin, L., Chavez, L.L., Li, D., Self, S.G., Perelson, A.S., 2010. Estimation of the initial viral growth rate and basic reproductive number during acute HIV-1 infection. J. Virol. 84, 6096–6102.
Saksena, N.K., Wu, J.Q., Potter, S.J., Wilkinson, J., Wang, B., 2008. Human immunodeficiency virus interactions with CD8+ T lymphocytes. Curr. HIV Res. 6, 1–9.
Sellon, D.C., Perry, S.T., Coggins, L., Fuller, F.J., 1992. Wild-type equine infectious anemia virus replicates in vivo predominantly in tissue macrophages, not in peripheral blood monocytes. J. Virol. 66, 5906–5913.
Sponseller, B.A., Sparks, W.O., Wannemuehler, Y., Li, Y., Antons, A.K., Oaks, J.L., Carpenter, S., 2007. Immune selection of equine infectious anemia virus env variants during the long-term inapparent stage of disease. Virology 363, 156–165.
Stafford, M.A., Corey, L., Cao, Y., Daar, E.S., Ho, D.D., Perelson, A.S., 2000. Modeling plasma virus concentration during primary HIV infection. J. Theor. Biol. 203, 285–301.
Taylor, S.D., Leib, S.R., Carpenter, S., Mealey, R.H., 2010. Selection of a rare neutralization-resistant variant following passive transfer of convalescent immune plasma in equine infectious anemia virus-challenged SCID horses. J. Virol. 84, 6536–6548.
Taylor, S.D., Leib, S.R., Wu, W., Nelson, R., Carpenter, S., Mealey, R.H., 2011. Protective effects of broadly neutralizing immunoglobulin against homologous and heterologous equine infectious anemia virus infection in horses with severe combined immunodeficiency. J. Virol. 85, 6814–6818.
Vaidya, N.K., Ribeiro, R.M., Miller, C.J., Perelson, A.S., 2010. Viral dynamics during primary simian immunodeficiency virus infection: effect of time-dependent virus infectivity. J. Virol. 84, 4302–4310.
Valli, V.E., 2007. Veterinary Comparative Hematopathology, 1st ed. Blackwell Pub, Ames, Iowa.
Wu, H., Zhu, H., Miao, H., Perelson, A.S., 2008. Parameter identifiability and estimation of HIV/AIDS dynamic models. Bull. Math. Biol. 70, 785–799.
Wu, W., Blythe, D.C., Loyd, H., Mealey, R.H., Tallmadge, R.L., Dorman, K.S., Carpenter, S., 2011. Decreased infectivity of a neutralization-resistant equine infectious anemia virus variant can be overcome by efficient cell-to-cell spread. J. Virol. 85, 10421–10424.